Electronic Supplementary Information

Molecular recognition and potentiometric determination of neostigmine and pyridostigmine by a methylene-bridged naphthotube

Jian-Fang Wu,[‡a,b] Wen-Jie Chen,[‡b] Li-Li Wang,[b] Liu-Pan Yang,[b] Yan-Fang Wang*[c] and Dehua Liao*[a]

[a.] *Department of Pharmacy, Hunan Cancer Hospital, the Affiliated Cancer Hospital of Xiangya School of Medicine, Central South University, Changsha, Hunan 410000, China. E-mail: liaodehua1125@126.com*

[b.] *School of Pharmaceutical Science, Hengyang Medical School, University of South China, Hengyang, Hunan, 421001, China; *E-mail: yanglp@usc.edu.cn.*

[c.] *Department of Chemistry, Zhejiang University, Hangzhou310058, P. R. China; ZJU-Hangzhou GlobalScientific and Technological Innovation Center, ZhejiangUniversity, Hangzhou 311215, P. R. China. E-mail: 11930562@mail.sustech.edu.cn*

Table of Contents

1. General Methods

1.1. General. All the reagents and guest molecules involved in this research were commercially available and used without further purification unless otherwise noted. Solvents were either employed as purchased or dried prior to use by standard laboratory procedures. Specifically, neostigmine bromide, pyridostigmine bromide, and poly(3,4-ethylenedioxythiophene)-poly(styrenesulfonate) (PEDOT:PSS) were purchased from Shanghai Bide Pharmatech Co., Ltd (China). Sodium tetrakis[3,5-bis(trifluoromethyl)phenyl]borate (NaTFPB), iron(III) chloride hexahydrate, ammonium chloride, and other inorganic salts were obtained from Energy Chemical (China). Solvents including dichloromethane, petroleum ether, and tetrahydrofuran were acquired from Shanghai Titan Scientific Co., Ltd (China). ^{1}H NMR, Diffusion-Ordered Spectroscopy (DOSY) and Rotating Overhauser Effect Spectroscopy (ROESY) were recorded on a Bruker Avance-500 NMR spectrometer at 25 ^{o}C. Electrospray-ionization high-resolution mass spectrometry (ESI-HRMS) experiments were conducted on an applied Q EXACTIVE mass spectrometry system. High-performance liquid chromatography (HPLC) analyses were conducted on a Shimadzu LC-20ADXR system. Elemental analyses (EA) were carried out with an Elementar Vario EL cube elemental analyzer through the Scientific Hound testing platform. Electrochemical measurements were implemented using a CHI660E electrochemical workstation (Shanghai Chenhua Instrument Co., Ltd.). Ultrapure water was purified from Chuangchun pure water machine CCH-H200.

1.2. HPLC Experiment

H1 was dissolved in a dichloromethane solution (1.0 mM), filtered through a 0.22 μm organic membrane. The chromatographic conditions are as follows: the stationary phase was an ArtChiral®Amy-S column (250 mm × 4.6 mm, 5 μm), and the mobile phase was isopropanol/hexane (v/v = 20:80) with a flow rate of 1.0 mL·min^{-1}. The column temperature was set at 40 °C, and the injection volume was 10.0 μL. The purity of the target compound was continuously monitored at a wavelength of 254 nm, with a system equilibrium time of 30 minutes and a total run time of 60 minutes.

1.3. ^{1}H-NMR titration

^{1}H-NMR titration was performed using a Bruker Avance-500 spectrometer. **H1** (0.5 mM) was titrated with **NEO** and **PYR** (10.0 mM), respectively. The concentrations of **NEO** and **PYR** were in the range of 0~2.06 mM, and the binding constants were obtained by nonlinear curve fitting through Origin 2019 or Musketeer software developed by Prof. Christopher A. Hunter's group at the University of Cambridge (Chem. Sci., 2024, 15, 15299).

1.4. Solid-state electrode pretreatment

The surface of the electrode is polished on suede with alumina polishing powder with a particle size of 0.05 μm. First, the electrode surface is rinsed with ultrapure water to remove the residual alumina, and then ultrasonic cleaned with ultrapure water and 50.0% ethanol solution for 30~60 seconds, and finally dried with cold air. After drying the electrode, 4 μL of the conductive polymer poly (3-ethylenedioxythiophene)-poly (styrene sulfonic acid) was applied to the surface of the electrode using a liquid transfer gun. The coated electrode is then dried for 12 hours.

1.5. Fabrication of membrane sensors

The sensor membrane for **NEO** and **PYR** selective electrodes was prepared by thoroughly mixing NaTPB (1.6 wt%), PVC (33.0 wt%), NPOE (63.4 wt%), and **H1** (2.00 wt%) and dissolving them in 1 mL of tetrahydrofuran (THF) to form a uniform solution. The mixture was subjected to vigorous ultrasonication in a bath for several h to ensure complete dissolution and uniformity. Subsequently, the solution was placed in a refrigerator for 4 h to form a stable and uniform membrane solution. Then, 20 μL of the well-mixed membrane solution was carefully dispensed onto the surface of the electrode using a micropipette. The electrode was then placed in a dust-free environment and allowed to dry overnight at room temperature to ensure the complete evaporation of the solvent and the formation of a uniform membrane. Before use, the electrode membrane was soaked in a 1×10^{-2} mol L^{-1} testing solution for 24 h. This step is crucial for the proper activation of the membrane and ensures consistent performance. When not in use, the electrode was stored in the same testing solution to maintain its functionality and stability.

1.6. Calibration of the sensors

Prepare solutions of **NEO** and **PYR** at concentrations ranging from 10^{-8} to 10^{-2} mol L^{-1}. respectively. Subsequently, the prepared electrode was immersed in the above solution together with the Ag/AgCl reference electrode, and the system reached

equilibrium under continuous stirring. When the potential change stabilized to within ±1 mV, the potential value was recorded, and the curve between the potential and the negative logarithmic values of **NEO** and **PYR** concentrations was plotted accordingly.

1.7. Effect of pH

In order to achieve optimal experimental conditions for quantitative determination with ion-selective electrodes. The effect of pH on the response of the investigated electrodes was studied using 10^{-3} and 10^{-4} mol L^{-1} solutions of **NEO** in BRB with pH ranging from 2 to 11.

1.8. Sensor selectivity

The potentiometric selectivity coefficients$\left(K_{A.B}^{pot}\right)$ of the proposed sensors towards different substances were determined by a separate solution method using the following equation:

$$-log\left(K_{A.B}^{pot}\right) = \frac{E_1 - E_2}{2.303\ RT\ /\ Z_A F} + \left[1 - \frac{Z_A}{Z_B}\right] log\ a_A$$

where $\left(K_{A.B}^{pot}\right)$ is the potentiometric selectivity coefficient, E_1 is the potential measured in 10^{-3} mol L^{-1} **NEO** solution, E_2 is the potential measured in 10^{-3} mol L^{-1} interferent solution, Z_A and Z_B are the charges of NEO and interfering ion, respectively, a_A is the activity of the drug and $2.303\ RT/Z_A F$ represents the slope of the investigated sensors (mV/concentration decade).

1.9. Determination of NEO and PYR in fetal bovine serum

One milliliter of each of 10^{-2}, 10^{-3} and 10^{-4} mol L^{-1} NEO solution were added separately into three 20 mL stoppered shaking tubes each containing 9 mL of fetal bovine serum and the tubes were shaken for 1 min. The membrane sensors were immersed in conjunction with the reference electrode in these solutions and washed with water between measurements. The emf produced for each solution was measured by the proposed sensors, and the concentration of **NEO** was determined from the corresponding regression equation. Fetal bovine serum **PYR** was determined by the same method.

1.10. Determination of NEO in pharmaceutical preparations

Pour 0.5 mg per milliliter of neostigmine methylsulfate injection into a 50 mL volumetric flask, and then the volume was completed with doubly distilled water. The concentration of the prepared samples was 10^{-4} mol L^{-1}. The potentiometric measurements were performed using the investigated sensors in conjunction with the reference electrode, and the potential readings were compared to the calibration plots.

1.11. Determination of PYR in pharmaceutical preparations

For analysis of Pyridostigmine Bromide Tablets tablets, 20 tablets were weighed and ground to fine powder and an appropriate weight from this powder was taken and was mixed with 50 mL doubly distilled water, shaken in a mechanical shaker for about 30 min and filtered into a 100 mL volumetric flask, then the volume was completed with doubly distilled water. The concentration of the prepared samples was 10^{-4} mol L^{-1}. The potentiometric measurements were performed using the investigated sensors in conjunction with the reference electrode, and the potential readings were compared to the calibration plots.

1.12. Statistical Analysis

All experiments were performed in triplicate unless otherwise specified. Data are presented as mean ± standard deviation (SD). Selectivity coefficients were calculated using the separate solution method (SSM) according to IUPAC guidelines.

2. Synthetic procedure

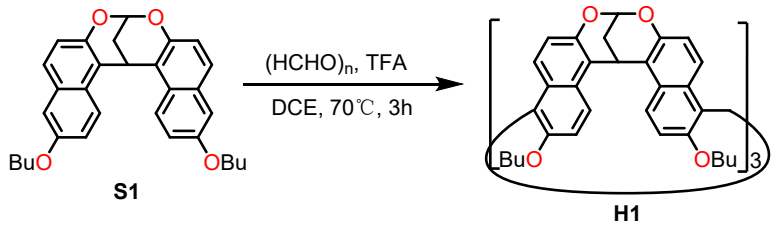

To a 500 mL two-necked flask, alkoxy-substituted bisnaphthalene clefts (**S1**) (1.0 mmol), paraformaldehyde (37.5 mg, 1.3 mmol), tetraethyl ammonium bromide (210 mg, 1.0 mmol) and dry 1,2-dichloroethane (DCE, 200 mL) were added. After stirring at 70 °C under Ar atmosphere for 1 h, trifluoroacetic acid (1.6 ml, 20.0 mmol) in dry DCE (30 mL) was added dropwise throughout ca. 30 min, and the resulting mixture was stirred at 70 °C for 3 h. Subsequently, the solvent was removed under reduced pressure. The residue was dissolved in CH_2Cl_2 (50 mL) and the mixture was washed with a saturated aqueous solution of NaHCO3 (50 mL). The organic phase was concentrated to give a yellow solid. The crude was purified by column chromatography (Al_2O_3, hexane/dichloromethane = 1/3) to give pure **H1** (42 mg, 9%). ^{1}H NMR (500 MHz, Methylene Chloride-d_2) δ 8.36 (d, J = 9.3 Hz, 2H), 8.28 (d, J = 9.3 Hz, 2H), 8.18 (d, J = 9.3 Hz, 2H), 8.09 (d, J = 9.2 Hz, 2H), 7.94 (d, J = 9.3 Hz, 2H), 7.76 (d, J = 9.3 Hz, 2H), 7.34 (d, J = 9.3 Hz, 2H), 7.29 (d, J = 9.3 Hz, 2H), 7.06 (d, J = 9.2 Hz, 2H), 6.91 (d, J = 9.3 Hz, 2H), 6.83 (d, J = 9.2 Hz, 2H), 6.72 (d, J = 9.3 Hz, 2H), 6.10 (s, 2H), 6.00 (s, 1H), 5.16 (s, 2H), 5.04 (s, 1H), 4.96 (d, J = 15.4 Hz, 1H), 4.88 – 4.65 (m, 4H), 4.31 – 4.16 (m, 6H), 4.16 – 4.08 (m, 2H), 4.02 – 3.91 (m, 2H), 3.89 – 3.79 (m, 2H), 3.67 (d, J = 8.0 Hz, 2H), 2.36 (d, J = 13.0 Hz, 2H), 2.23 – 2.12 (m, 2H), 2.07 (d, J = 2.7 Hz, 2H), 2.00 – 1.89 (m, 4H), 1.73 (td, J = 6.8, 2.7 Hz, 4H), 1.64 (q, J = 7.5 Hz, 4H), 1.52 – 1.40 (m, 8H), 1.13 (dt, J = 13.6, 6.8 Hz, 4H), 1.03 (t, J = 7.4 Hz, 6H), 0.97 (t, J = 7.4 Hz, 6H), 0.68 (t, J = 7.4 Hz, 6H). Anal. Calcd. for $C_{96}H_{96}O_{12}$: C, 79.97; H, 6.71. Found: C,78.49; H,6.75%. HPLC (iPrOH/n-hexane = 20/80, flow rate = 1.0 mL/min, λ = 254 nm) tR =9.1 min.

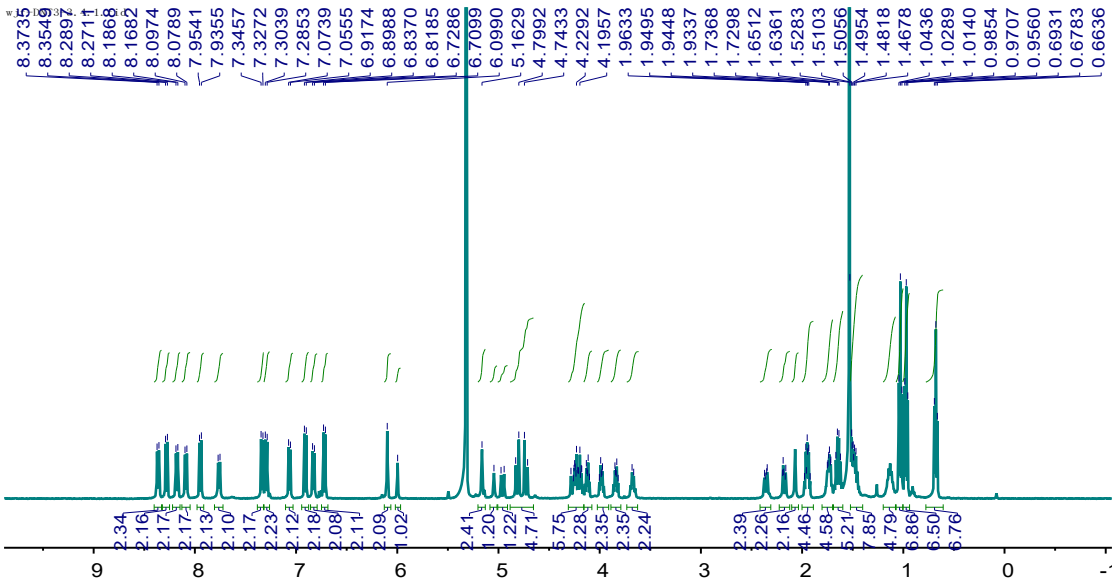

^{1}H NMR spectrum (500 MHz, CD_2Cl_2, 298 K) of **H1**

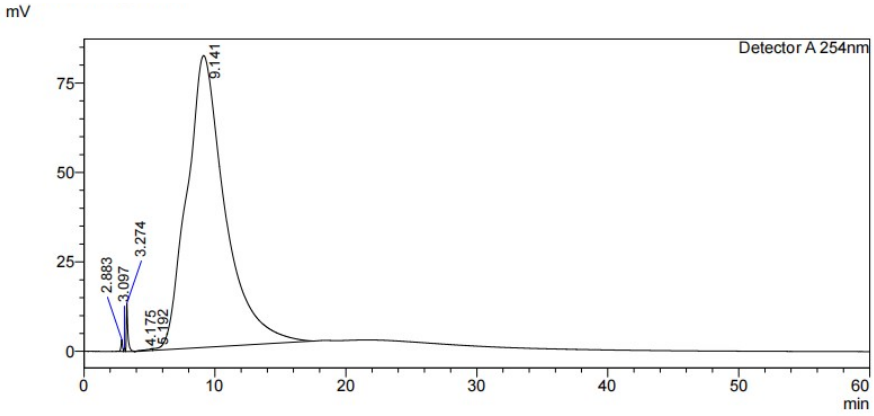

<Peak Table>

Detector A 254nm

Peak#	Ret. Time	Area	Height	Conc.	Unit	Mark	Name
1	2.883	25085	3335	0.150			
2	3.097	5722	857	0.034		V	
3	3.274	110273	13475	0.661		V	
4	4.175	2400	162	0.014			
5	5.192	18234	505	0.109		V	
6	9.141	16519743	81573	99.031		V	
Total		16681457	99907				

HPLC spectrum of **H1**

2. Host-Guest Binding Experiments

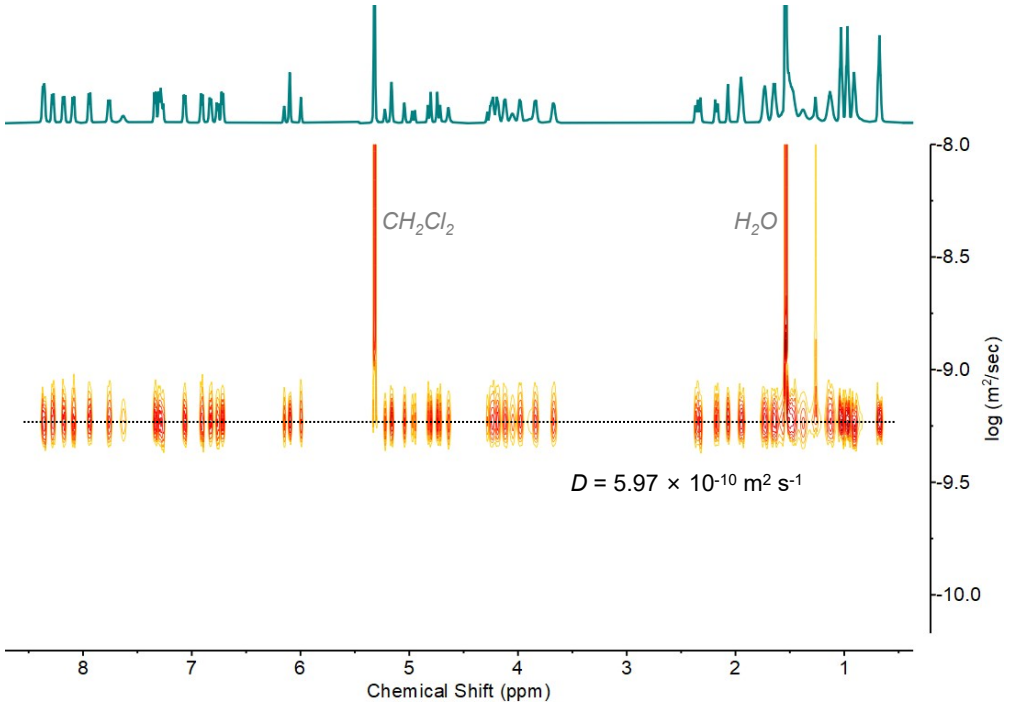

Fig. S1. DOSY NMR spectra (500 MHz, CD_2Cl_2, 298 K) of **H1** (2.0 mM). The diffusion coefficient was calculated to be 5.97×10^{-10} m^{2}s^{-1}.

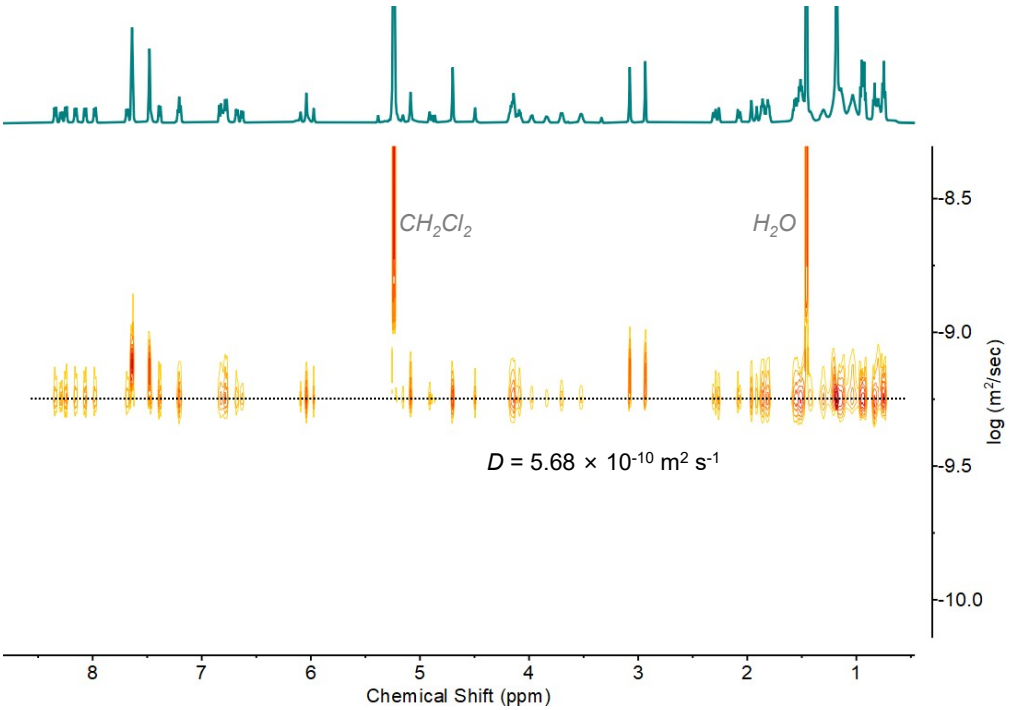

Fig. S2. DOSY NMR spectra (500 MHz, CD_2Cl_2, 298 K) of **NEO@H1** (2.0 mM). The diffusion coefficient was calculated to be 5.68 ×10^{-10} m^{2}s^{-1}.

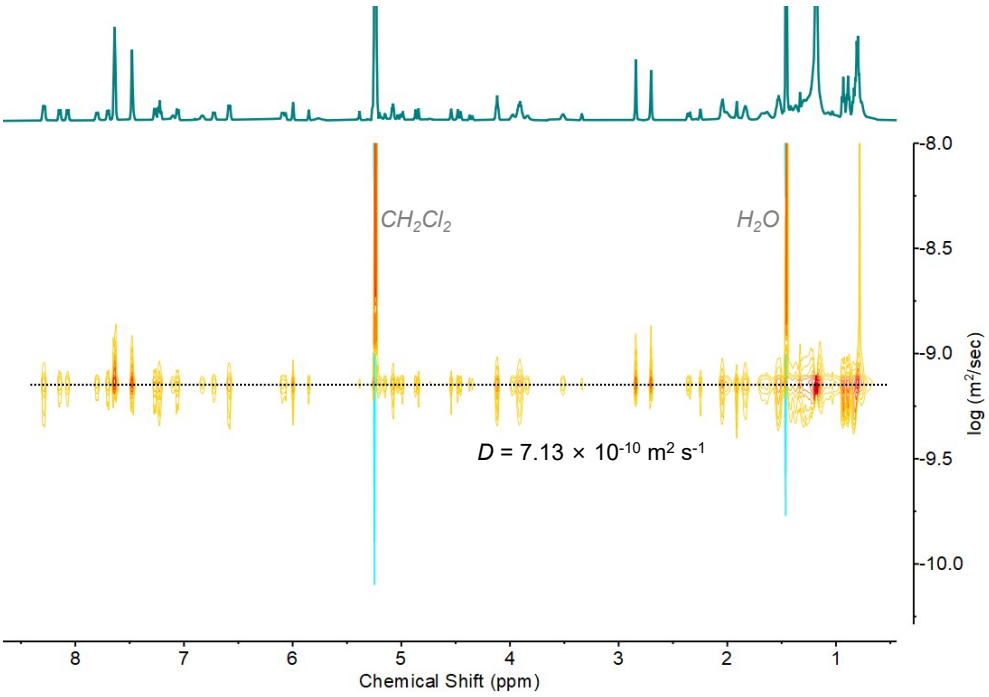

Fig. S3. DOSY NMR spectra (500 MHz, CD_2Cl_2, 298 K) of **PYR@H1** (2.0 mM). The diffusion coefficient was calculated to be 7.13×10^{-10} m^2s^{-1}.

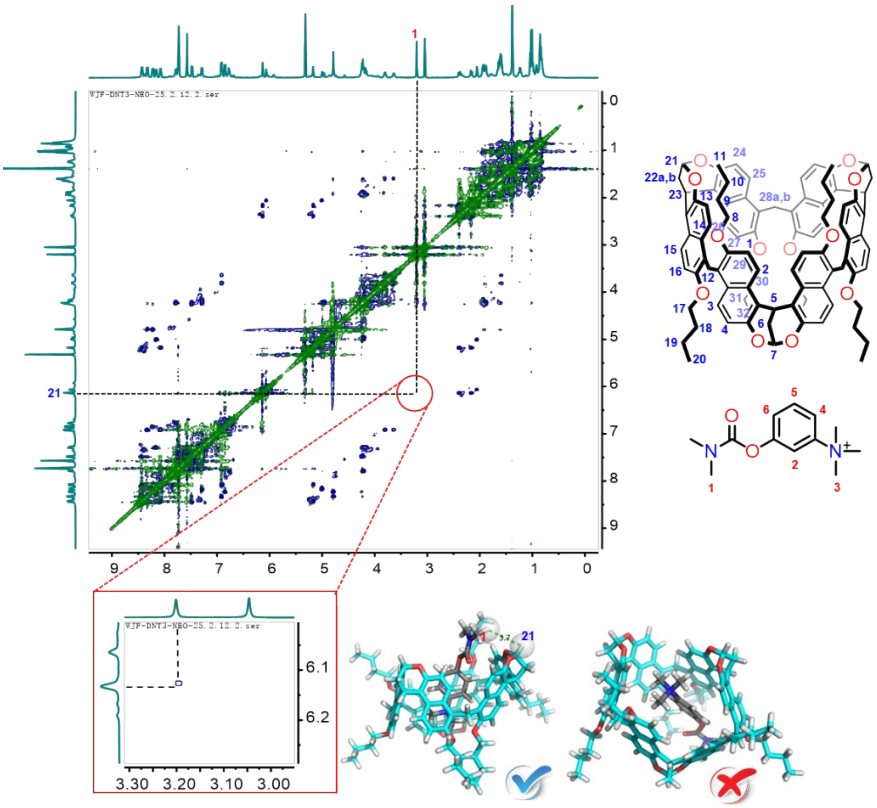

Fig. S4. ^{1}H, ^{1}H-ROESY NMR spectra (500 MHz, CD_2Cl_2, 298 K) of **NEO@H1** (6.0 mM) and energy-minimized structures of two possible conformers. Due to the fast exchange of the host-guest system on the NMR timescale, most guest signals disappeared into the baseline. We

therefore determined the molecular orientation of the guest within the cavity by observing NOE effects between the protons of the guest's *N*-methyl group and host protons. The data revealed NOE correlations specifically between the *N*-methyl protons and H21 (not H7) of the host, confirming the guest orientation as illustrated above.

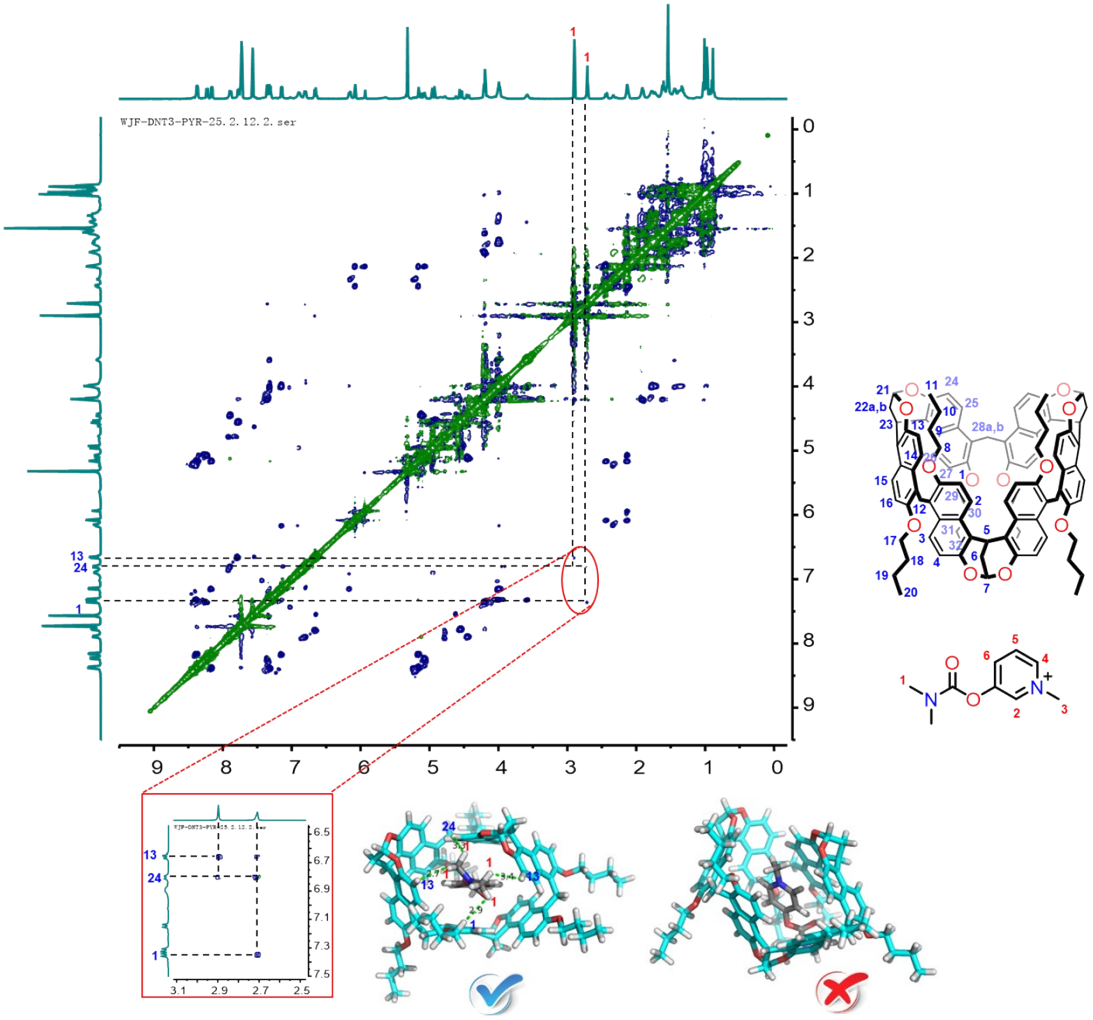

Fig. S5. ^{1}H, ^{1}H-ROESY NMR spectra (500 MHz, CD_2Cl_2, 298 K) of **PYR@H1** (6.0 mM) and energy-minimized structures of two possible conformers. Due to the fast exchange of the host-guest system on the NMR timescale, most guest signals disappeared into the baseline. We therefore determined the molecular orientation of the guest within the cavity by observing NOE effects between the protons of the guest's *N*-methyl group and host protons. The data revealed NOE correlations specifically between the *N*-methyl protons and H1, H24, H13 of the host, confirming the guest orientation as illustrated above.

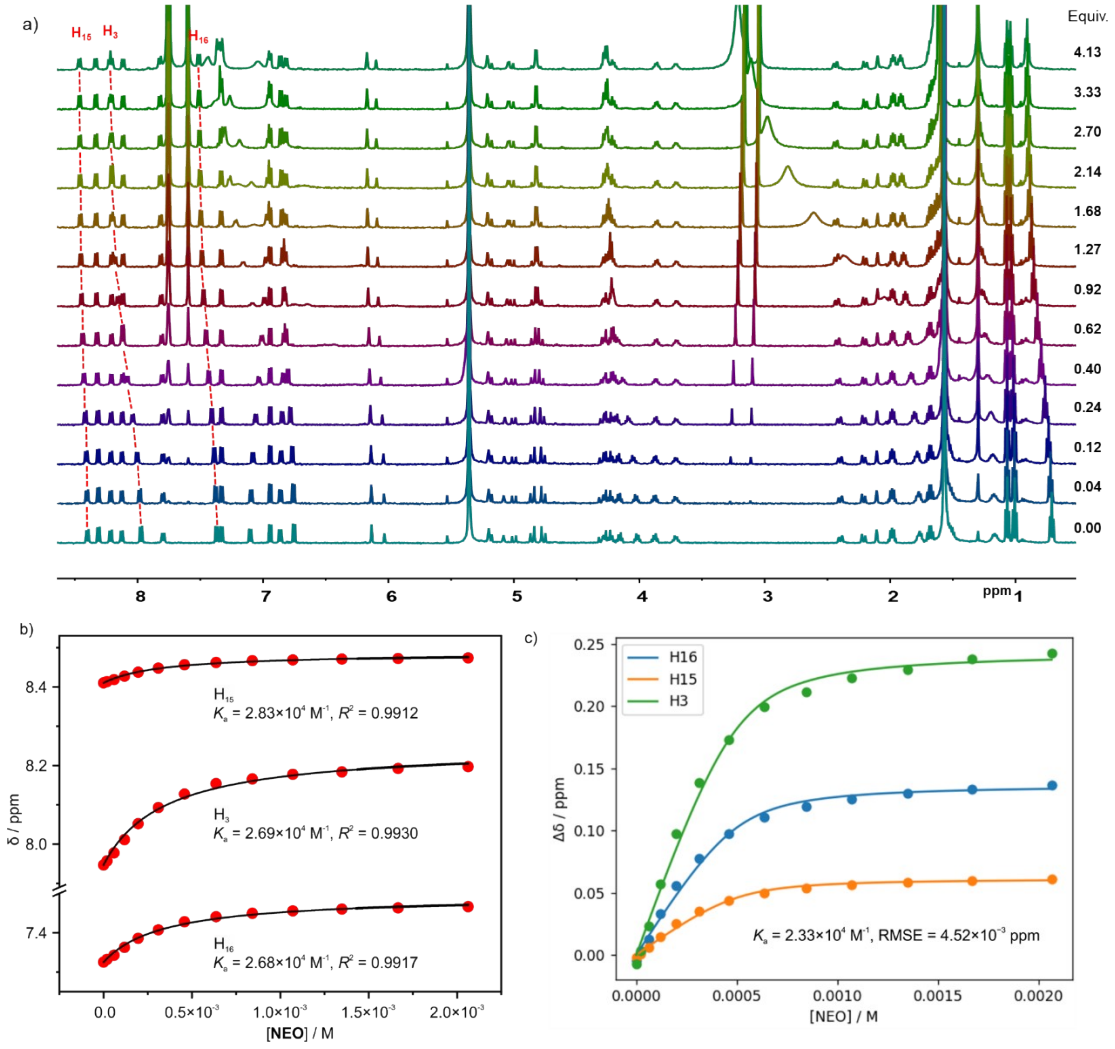

Fig. S6. (a) Full ^{1}H NMR spectra (500 MHz, CD_2Cl_2, 298 K) of **H1** titrated with different concentrations of **NEO**. The non-linear fitting of three proton signals against concentrations of **NEO** using a 1:1 binding model with Origin 2019 (b) or Musketeer software (c). The full NMR titration spectra reveal differential chemical shift changes of the host protons (upfield or downfield), demonstrating distinct shielding/deshielding effects on specific hydrogen positions due to the asymmetric guest. This spatial heterogeneity, arising from varied proximity to the guest's electron-rich/poor regions, confirms the orientation-dependent modulation of the host's electronic environment.

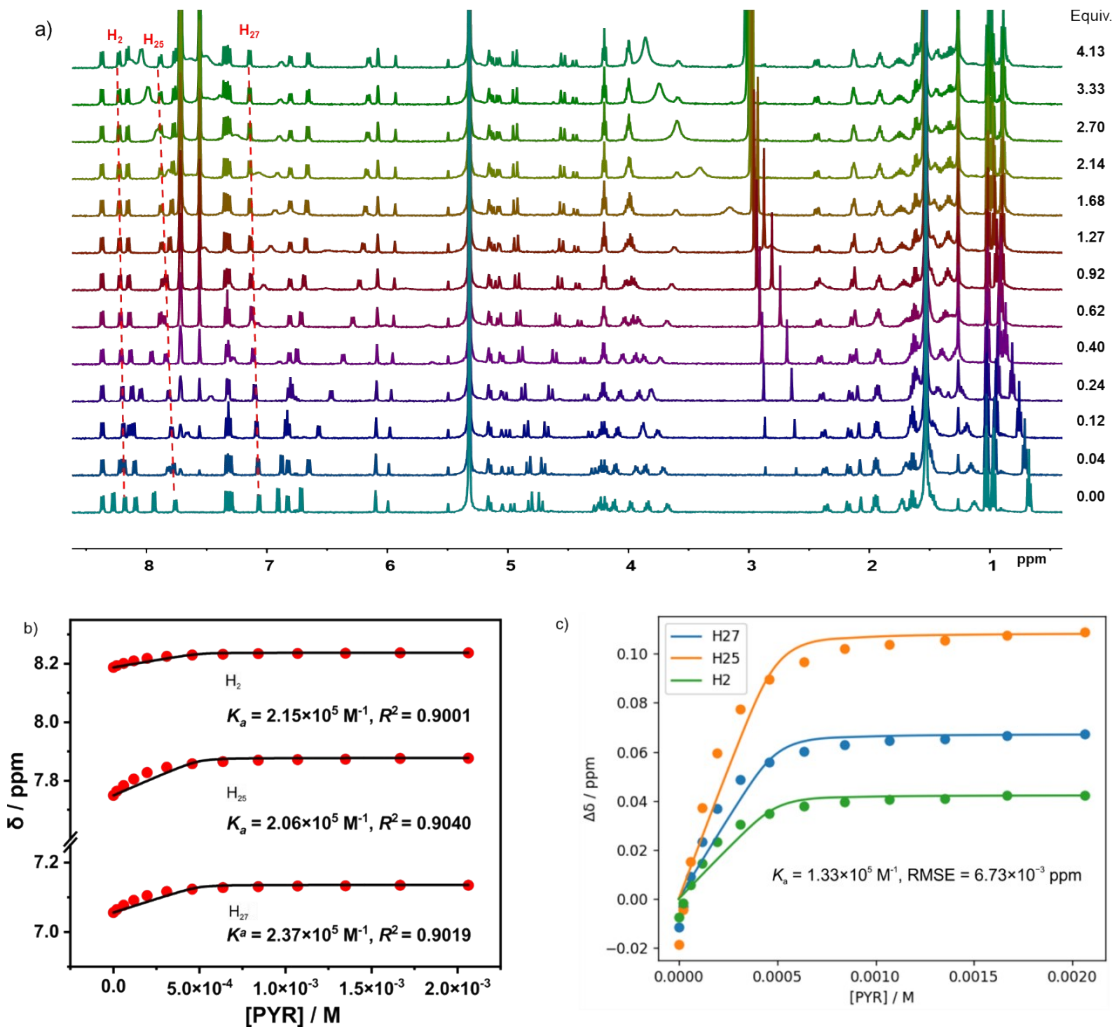

Fig. S7. (a) Full ^{1}H NMR spectra (500 MHz, CD_2Cl_2, 298 K) of **H1** titrated with different concentrations of **NEO**. The non-linear fitting of three proton signals against concentrations of **NEO** using a 1:1 binding model with Origin 2019 (b) or Musketeer software (c). The full NMR titration spectra reveal differential chemical shift changes of the host protons (upfield or downfield), demonstrating distinct shielding/deshielding effects on specific hydrogen positions due to the asymmetric guest. This spatial heterogeneity, arising from varied proximity to the guest's electron-rich/poor regions, confirms the orientation-dependent modulation of the host's electronic environment.

4. Electrochemical experiment

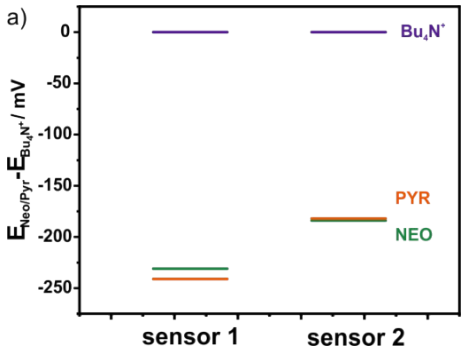

Fig. S8. The EMF values of ISEs containing diverse ionophores exposure to 1.0 mM **NEO** and **PYR** cation subtracted the corresponding EMF value.

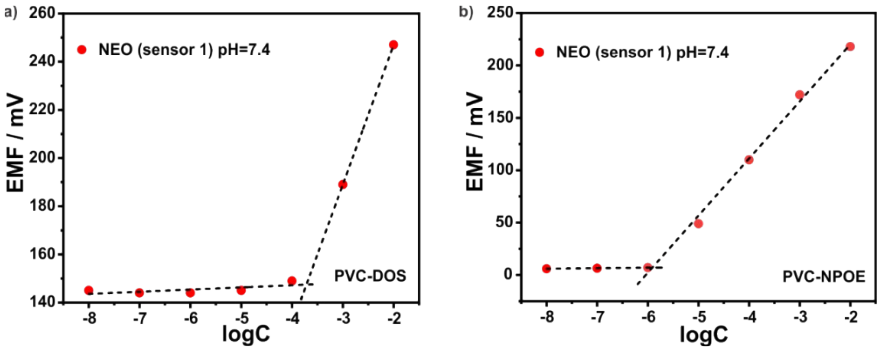

plasticizer	LOD (M)	Slope (mV/dec^{-1})	Linear range	R^2
DOS	1.9×10^{-4}	49.00±1.25	10^{-4}-10^{-2}	0.994
NPOE	1.5×10^{-6}	54.60±0.40	10^{-6}-10^{-2}	0.995

Fig. S9. By using different membrane plasticizers (a) DOS and (b) NPOE, the electromotive response of different concentrations of NEO cations in pH 7.4 BRB buffer solution was measured, and a calibration curve was plotted.

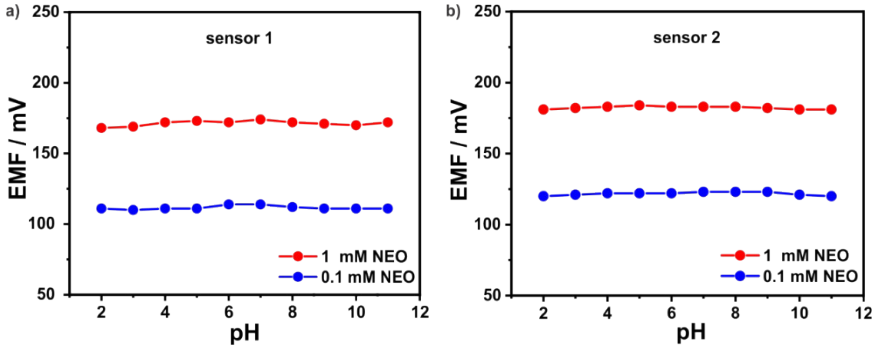

Fig. S10. Effect of pH on the response of (a) sensors 1 and (b) sensors 2 using 10^{-3} M and 10^{-4} M of **NEO**.

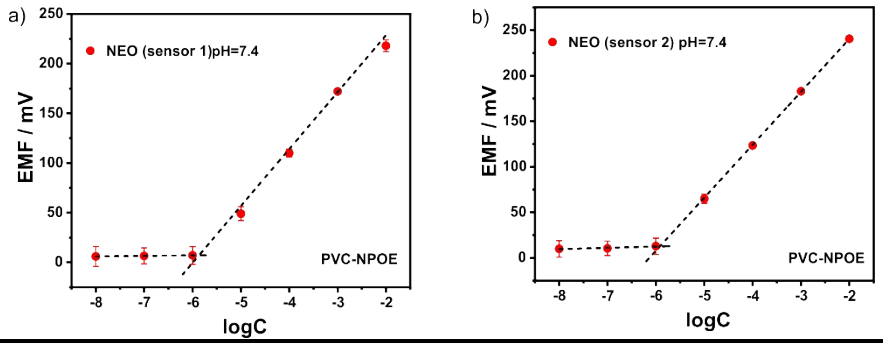

Ionophore	LOD (M)	Slope (mV/dec^{-1})	Linear range	R^2
Blank	1.5×10^{-6}	54.60±0.40	10^{-6}-10^{-2}	0.996
H1	1.3×10^{-6}	58.52±0.52	10^{-6}-10^{-2}	0.997

Fig. S11. Calibration curves of EMF responses to different concentrations of **NEO** cation for electrode without ionophore (a) Blank-based electrode (b) **H1**-based electrode.

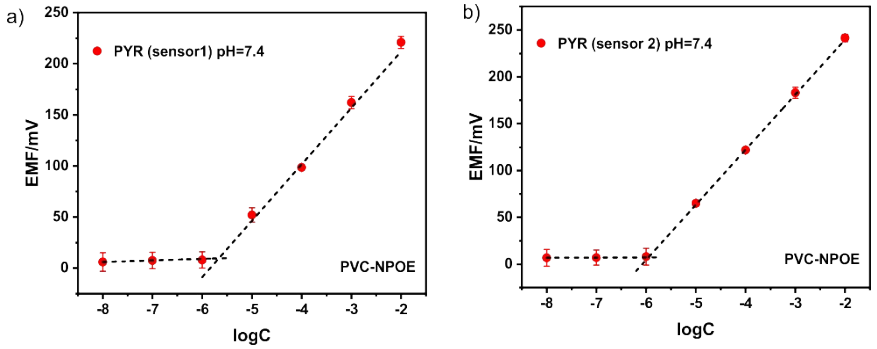

Ionophore	LOD (M)	Slope (mV/dec^{-1})	Linear range	R^2
Blank	1.4×10^{-6}	53.60±0.65	10^{-6}-10^{-2}	0.996
H1	1.0×10^{-6}	58.50±0.40	10^{-6}-10^{-2}	0.999

Fig. S12. Calibration curves of EMF responses to different concentrations of **PYR** cation for electrode without ionophore (a) Blank-based electrode (b) **H1**-based electrode.

Table S1. The selectivity coefficients for Na^+, K^+, NH_4^+, Fe^{3+}, Proline, histidine, and Glycine of the electrodes with (Sensor 2) or without **H1** (Sensor 1) as the ionophore. All interferents are in the form of 1×10^{-3} mol L^{-1} solution.

Analytes	Sensor 1 $log(K\frac{pot}{A.B})$	Sensor 2 $log(K\frac{pot}{A.B})$
Na^+	-2.3±0.41	-2.9±0.37
K^+	-2.4±0.33	-2.8±0.25
NH_4^+	-2.5±0.51	-3.0±0.37
Fe^{3+}	-2.9±0.57	-3.3±0.41
Proline	-2.9±0.59	-3.6±0.57
histidine	-2.8±0.57	-3.3±0.49
Glycine	-2.8±0.75	-3.2±0.41

Table S2. Determination of **NEO and PYR** in real samples

Sample	Added(μmol L^{-1})	Found[a](μmol L^{-1})	Recovery (%)±S.D.
PYR	100	99.0	99.0±1.8
NEO	100	99.0	99.0±1.9

[a] Mean value (n = 3).